Automated Detection of Microaneurysm for Fundus Images

Norhasmira Mohammad[1], Zaid Omar[2], Eko Supriyanto[1]
[1]Faculty of Biosciences and Medical Engineering
[2]Faculty of Electrical Engineering
Universiti Teknologi Malaysia
81310 Johor, Malaysia.

Alexander Dietzel[3], Jens Haueisen[3]
[3]Institute of Biomedical Engineering and Informatics
Technical University of Ilmenau
98684 Ilmenau, Germany.

***Abstract*— Chronic hyperglycemia of diabetes may lead to failure in various organs, especially the blood vessels, eyes, kidneys, nerves and heart. It happens due to the faults either in insulin secretion, insulin action, or both. As diabetes developed, the vision of patient starts to deteriorate, leading to Diabetic Retinopathy (DR). Microaneurysm (MA) are the earliest sign of DR where it appears in clusters as tiny, dark red spots or tiny hemorrhages-like within the retina light-sensitive area. Thus, the objectives of this study are to develop an automated algorithm to perform early detection of MA presence in fundus images, and to evaluate the performance of the proposed system design by evaluating the accuracy of the segmented MA. The methods involved in the pre-processing stage are the green component extraction and bottom hat filtering with gamma correction. As the characteristics of blood vessel and MA are the same, the extraction of vessels is needed. This is done by applying the Gaussian matched filter. It is then segmented out by using certain threshold value. In template learning, wavelet coefficient is used in separating the pattern and background image by following the Gaussian distribution curve. Texture energy filter is used to extract the true features where MA are identified. As a result, 84.15% of accuracy is obtained.**

Keywords—Diabetic Retinopathy; Microaneurysms; Detection; Segmentation.

I. INTRODUCTION

Diabetic retinopathy (DR) is quite common for person with diabetes, where it grows over time and the patients themselves should undergo treatments in order to control the progression of the disease which may cause damage to the retina, a thin layer of light-sensitive tissue that lines at the back of the eye [1]. It is a serious complication that may affect the eyesight of diabetic patients. The main cause of DR is due to high glucose level in blood which will eventually affect the vascular walls where MA starts to appear. However, the presence of this abnormality does not affect the vision itself, but progression of DR to later stages leads to complications such as progression of new vessels and macular edema. Thus, this problems may lead to vision impairment and blindness. About 2% of the diabetic patients are reported blind and 10% suffer from vision loss after 15 years of diabetes due to DR complications [2].

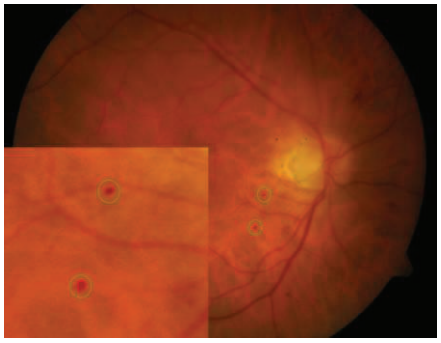

Figure 1 Microaneurysms in the fundus image of a diabetic patient

World Health Organization has stated that 366,000,000 people will be affected by diabetes in 2030 [3]. As the number of patients increases over the time, large number of experts or ophthalmologists are required to examine the patients. Thus, regular checkup is highly recommended in order to reduce the progression of DR and as a prevention to vision loss.

There are three stages of DR which are Non-proliferative Diabetic Retinopathy (NPDR), Proliferative Diabetic Retinopathy (PDR) and Severe Diabetic Retinopathy (SDR). NPDR is the initial stage of DR where the arteries in the retina become weak and start to leak, forming small, dot-like bodies called hemorrhages. In PDR stage, new fragile blood vessels are developed as the circulatory system tries to maintain appropriate oxygen levels within the retina. Blood may leak into the retina and vitreous, causing spots or floaters, together with decreased vision. In SDR stage, the retinal detachment occurred and patients will have a high possibility to have glaucoma and gradual loss of vision due to continuously growing of abnormal vessels and scar tissues. Figure 1 shows the example of MA in clusters as tiny, dark red spots or tiny hemorrhages-like within the retina light-sensitive area. Their sizes range from 10-100 microns and are circular in shape [4].

II. APPLICATION OF DIGITAL IMAGE PROCESSING IN FUNDUS IMAGES

Nowadays, digital image processing is widely used in order to examine the interesting lesions in DR. It is very useful for detection of the initial signs of DR. There are various

978-1-4673-7791-1/16/$31.00 ©2016 IEEE

approaches introduced by researchers in enhancing the features of the DR images, segmenting the region of interest and classifying the lesions. Recently, a study in early detection of MA is conducted [5]. A lesion detection is proposed using retinal fundus image together with the analysis in blood vessel removal by using Naïve-Bayes classifier. They obtained 88% of sensitivity approximately. However, in [3], by using kernel density estimation with variable bandwidth in classification stage they managed to obtain 88.5% of sensitivity.

In [6], an automated MA detection using local contrast normalization and local vessel detection has been proposed where they used k-nearest neighbor (kNN) classifier to classify the MA. They manage to obtained sensitivity of 85.4% and specificity of 83.1%. In [7], a multilayer perceptron (MLP) classifier is subsequently used to obtain the final segmentation of red lesions. As a result, by using lesions characteristics, they obtained mean sensitivity of 86.1% and a mean positive predictive value of 71.4%. With an image-based criterion, 100% mean sensitivity, 60.0% mean specificity and 80.0% mean accuracy are obtained.

In other research [8], the authors have designed an algorithm for extracting the hemorrhages using template matching with various shapes of template where the percentage of the system sensitivity obtained is 85% at 4.0 false positive per image. Furthermore, in [9], the authors have introduced the abnormalities detection of fundus images where in pre-processing stage they proposed a method which has an ability to remove the noise and enhance the quality of the images. Contrast Limited Adaptive Histogram Equalization (CLAHE) is used to enhance the contrast of the image. Image correction is performed by subtracting the pre-processed images with green channel. Top hat transform is used as it has an ability to extract small elements and fine details from images. Black top hat transform is used to detect the retinal abnormalities. Adaptive Neuro Fuzzy Inference System (ANFIS) is a type of neural network that is used to classify the retinal images as normal, mild and severe DR. In this proposed method, they managed to obtain 66.67% of sensitivity, 62.5% of specificity and 63% of accuracy.

All present studies in the detection and classification of all candidates in DR fundus images are the improvement of previous studies. In this paper, an automated algorithm for detecting the earliest sign of DR is designed. A novel template algorithm named as Template Learning from Atomic Representations (TEMPLAR) is used for pattern learning and analysis [10]. On the other hand, the true features are extracted using texture energy filter where a 2D filter is formed. Finally, superimpose method is used to overlay the manual marked image and segmented MA.

III. METHODOLOGY

Figure 2 below shows the flowchart of the proposed method applied in this research. The selected sample of input images are analyzed first in order to identify the interest features of the image before entering the pre-processing stage.

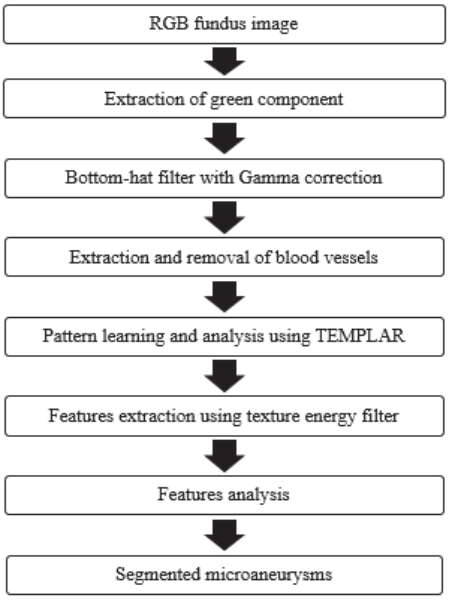

Figure 2 Steps of methodology

A. Pre-processing stage

RGB fundus images often suffer from non-uniform illumination, poor contrast and noise. Among these RGB channels, green channel gives the best contrast in fundus images, red channel often provides a saturated and has low contrast while blue channel is very noisy and suffers from poor dynamic range [11].

Bottom-hat transformation is essentially a combination of subtracted images with the opening and closing where opening image are referred to the decreasing in the intensity for all bright features and it is depending on the size of the features itself. However, closing image will attenuate the dark features while the background of the image will not be affected at all. Thus, bottom-hat transformation associated with gamma correction may provide promising output as it controls the overall brightness.

B. Extraction and removal of blood vessels

Characteristics of blood vessel in fundus images discussed in [11] are as follows; vessels can be approximated as anti-parallel segments, and vessels have lower reflectance than other retinal surfaces. They appear darker relative to the background. Vessel sizes may decrease when they are away from the optic disk, the width of a retina vessel may lie within the range of 2–10 pixels. Besides, the intensity profile varies by a small amount from vessel to vessel and it has a Gaussian shape.

In this stage, blood vessels are detected using matched filter based on their characteristics mentioned in the paragraph above. The importance of removing this feature is to preserve the area that contains MA and other lesions that have similar characteristics to the candidate. The idea of how this matched filter works is by assuming blood vessels often follow the Gaussian shape.

$$f(x,y) = A\{1\text{-}k\ exp(-d^2/2\sigma^2)\} \quad (1)$$

The equation above is the Gaussian curve equation where *d* is the perpendicular distance between any point of coordinate (x,y) and the straight line passing through the center of the blood vessel in a direction along its length, σ defines the dissemination of the intensity profile, A is the grey-level intensity of the local background, and k is the measure of reflectance of the blood vessel relative to its neighborhood. However, a significant improvement can be achieved by matching a number of cross sections of identical profile simultaneously. Thus, a kernel can be used with the mathematical expression as follows,

$$K(x,y) = -exp(-x/2\sigma^2) \quad \text{for } |y| \le L/2, \quad (2)$$

where L is the length of the segment for which fixed orientation has been assumed. To move this Gaussian-shaped filter along the blood vessel, different orientations of the kernel have been made. The rotation angle is 15º in each of the orientations. Convolution of the generated kernel with a vessel intensity profile function allows decision whether the pixel belongs to the vessel or not.

Furthermore, to perform this matched filtering algorithm in detecting the blood vessel and reducing the noise, an input image needs to undergo the low pass filter such as the simple one which is mean filter with 5x5 mask. Then, matched filter with a specific angle of the orientations is applied. The next step is the blood vessel removal by performing a thresholding method.

C. Pattern learning and analysis using TEMPLAR

A wavelet is a representation of mathematical model that is typically used in digital signal processing and image compression. This wavelet method is still be used over the time as the theory behind it still remains the same and it gives a promising output in certain analysis. The principles are similar to those of Fourier analysis, which was first developed in the early part of the 19th century [12]. In signal processing, wavelets manage to improve a weak signal that is exposed to noise. For example, most of the medical images have been successfully denoised using wavelets approaches such as x-ray, magnetic resonance imaging (MRI) and ultrasound.

In this research, the wavelet decomposition is performed in order to develop a wavelet-based statistical model for a training pattern. Template learning is being implemented to model a statistics wavelet coefficient whereas this coefficients are assumed to follow a two-state Gaussian mixture model (GMM) distribution locally. Besides, template learning is a learning process of the pattern stored in training dataset where in this case a number of MA samples is trained.

Template matching always come with a problem in the separation of the background from the pattern of interest and modelling the local deformation. Thus, in order to overcome this problem, Template Learning from Atomic Representation (TEMPLAR) algorithm [13] has been proposed.

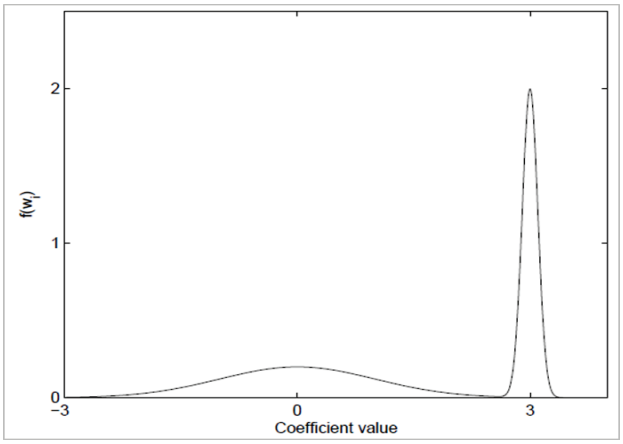

Figure 3 Two states Gaussian mixture model for template learning [12]

Generally, edges of the pattern represent the important information in any interest pattern. Therefore, TEMPLAR algorithm emphasizes the properties of edge detection in the wavelet transform. The significant coefficients that represent the edge pattern in an image are selected by introducing the Minimum Description Length (MDL) principle.

GMM used for modeling wavelet coefficients has the form that assumes two zero mean Gaussians; one with a low variance and the other with a high variance [13]. However, for template learning, different forms of GMMs need to be used because the local statistics of wavelet coefficient should be considered. This is the most important parameter that should be modeled efficiently so that pattern and background of the images can be distinguished clearly. Below is the function of the wavelet coefficient w_i, where in this case the GMM proposed two states of Gaussian model.

$$fw_i(w_i) = \sum_{m=1}^{M} p_{Q_i}(m) f_{w_i|Q_i}(w_i|Q_i = m) \quad (3)$$

In the equation above, the conditional density of wavelet coefficient is given as $fw_i|Q_i\ (w_i|Q_i=m) \sim \mathcal{N}\ (\mu_i, m, \sigma^2_i, m)$. The state $Q_i = 1$ represents a zero mean Gaussian and the state $Q_i=2$ represents the Gaussian with non-zero mean. Figure 3 shows an illustration of this Gaussian mixture model. The state Qi=1 models the background and smooth regions with a zero mean and common variance across the subband, whereas the state $Q_i=2$ corresponds to the pattern. In other word, $Q_i=1$ is referred to the low state while $Q_i=2$ represents the high state. EM algorithm is used to compute these two states of GMMs in template learning.

D. Features Extraction using texture energy filter

In this section, the image obtained from previous methodology is used for extracting the candidates. As we have discussed in previous section, there are two states of GMMs which represent both foreground and background where the foreground image represents the desired features.

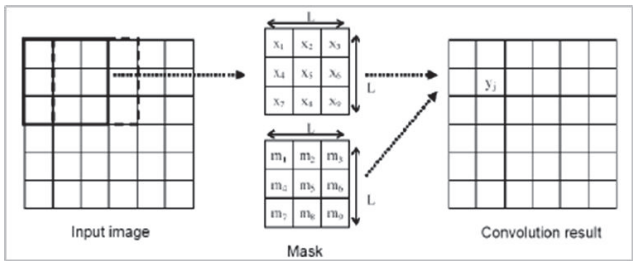

Figure 4 Mask convolution

However, the image still has some other noise which has similar properties with the actual candidate. Microstructures features are extracted based on ridges, edges, spots, waves, ripples and grooves.

Laws' convolution has been used for many applications of image analysis for classification and segmentation. The texture energy measurements for 2D images are computed by applying convolution filters. There are various lengths of filters that could possibly be used in texture energy measurement. Various lengths of vector can be used such as three, five, seven and nine.

The initial letters of each of 1-D vector is representing the local average (or Level), edge detection, and spot detection and the following numbers represent the length of the filter. Usually extended length of filter will be used in filtering the 2-D image. This is done by convolving the 1-D vector with the other vector which has the same length such as convolution of the L3 and E3. Thus, a 2-D filter with size of 3x3 can be formed. Examples of three basic filters are as follows:

L3 = (1 2 1)
E3 = (-1 0 1)
S3 = (-1 2 -1)

Besides, in [14] they have extended the length of 1-D filter to seven and nine. In this case, the same approach can be made. The 2-D filter can be formed by convolving the 1-D vector to obtain (5x5), (7 x 7) and (9 x 9) filter sizes.

The next step is the convolution of input image with the 2-D filter where the input image consists of M number of column and N number of row. Figure 4 shows the obtained 2-D filter. This filter is then used for calculating convolution by performing a convolution to the input image. The results of this convolution produce a greyscale image with a dimension of $N-window\ size+1 \times M-window\ size+1$ where window size can be 3 or 5, depending on filter size. Finally, image normalization is required for normalizing the size of output image so that it can be used for comparison with the original image size.

E. Features Analysis

In features analysis, the images obtained after performing the Laws' filter are compared to the original images where the manual marked region represents the MA. This is done by overlaying both images and statistical evaluation is made by calculating the true positive (TP) and false negative (FN) to compute the sensitivity of the system performance.

$$\text{Sensitivity} = \text{TP}\ (\text{TP}/\text{FN}) \quad (4)$$
$$\text{Accuracy} = \text{Sensitivity} \quad (5)$$

Where

TP is the number of MA that are correctly identified.
FN is the number of MA found as non-MA.

IV. RESULTS

Figure 6 shows the results of each of the methodology in order to detect the true MA candidates. The original fundus image in DIARETDB1 dataset which contains only MA is experimented in this automated algorithm. As the original fundus image is a color image, the extraction of green component is required for performing further analysis. Figure 5(a) shows the raw image and Figure 5(b) shows the output after the green component extraction. If we view this image thoroughly, we can clearly see that the MA candidates are more visible. Thus, green channel image is the most suitable to be used in further analysis as it offers more information compared to the other channels.

Figure 5(c) shows the detected blood vessels. As the vessels are assumed to follow the characteristic of Gaussian shape, the detection is done by moving the filter along the blood vessel with different orientations of the kernel. The selected angle is 15º for each orientation. Then, the result obtained is gone through the thresholding method in order to remove the blood vessels and preserve the round objects which may represent the MA candidates. The final result is shown in Figure 5(d).

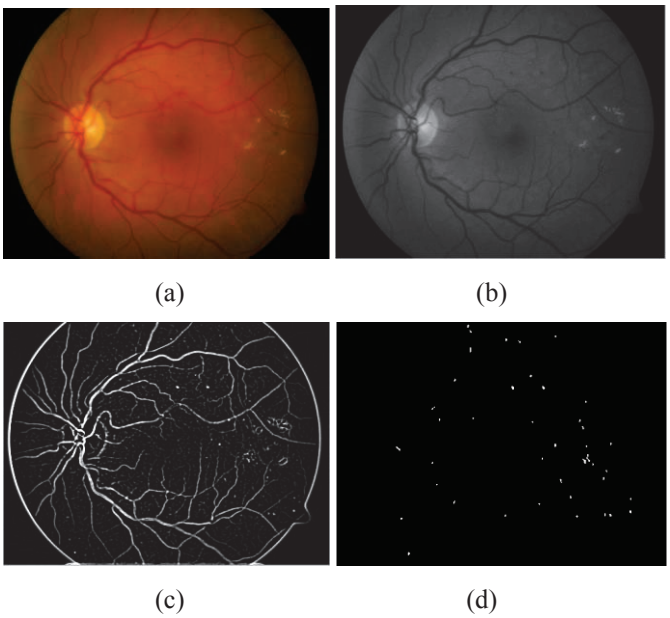

Figure 5 (a) Original fundus image and the images after (b) green channel extraction, (c) blood vessel detection and (d) microanuerysms segmentation

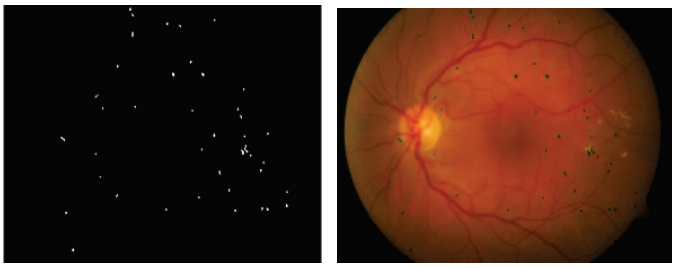

(a) (b)

Figure 6 (a) Segmented MA and (b) superimposed image of raw image and the segmented MA

In order to visualize the segmented MAs over the original image, we overlaid the binary image of segmented MAs with the original image. Figure 6 shows the superimposed result. In order to obtain the accuracy and sensitivity of the automated algorithm in detecting the MAs, statistical evaluation has been made.To perform the evaluation, ten fundus images are experimented in this automated algorithm. Analysis 1 until analysis 10 represent the number of images where the first analysis contributes large amount of MA candidates. As the number of analysis increases, the number of candidates in image also decreases. All images are taken from DIARETDB1 datasets which contain at least mild non-proliferative DR.

Based on the evaluation shown in Table 1, we can see that 95% of MA is detected on analysis 1 while analysis 10 gives the lowest percentage in detecting the MA which is 70.83%. The result of the calculated FP value shown in the analysis 3 contributed a very high percentage which is 78.57% while analysis 8 and 9 give zero percentage. As the original image of analysis 3 consists of large number of MA, an automated algorithm detects a significant amount of MA where almost half of the segmented MA are falsely detected. However, for analysis 8 and 9, the algorithm managed to detect exact number of MA as the original images only contain a few number of MA. Thus, the probability of the algorithm to detect the wrong MA is less.

Table 1 Percentage Of Evaluation

Analysis	TP (%)	FN (%)
1	95	5
2	92.86	7.14
3	91.67	8.33
4	90.91	9.1
5	83.33	16.67
6	83.33	16.67
7	80.77	19.23
8	77.78	22.22
9	75	25
10	70.83	29.17

Figure 7 shows the average percentage of TP which is 84.15% while the percentage of FN is 15.85%. Therefore, the higher the percentage of TP, the higher the sensitivity achieved. Low percentage of FN indicates a good performance of the system designed.

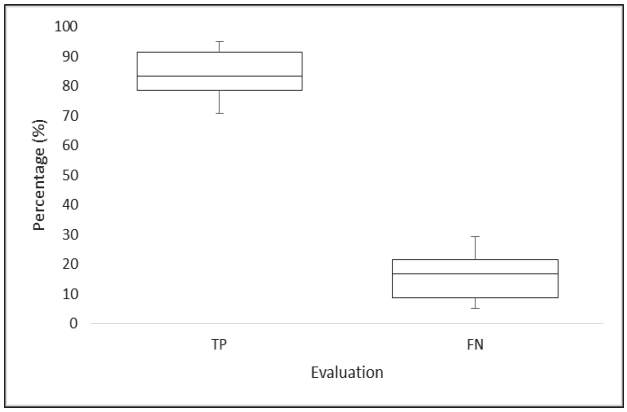

Figure 7 Average percentage of true positive and false negative

V. DISCUSSION

Ten images are selected to undergo the whole process of the proposed method. Due to the unavailability of the ground truth images, the candidates' marking process is done manually by plotting the position of MA in 2D binary image. Therefore, only a few number of images are selected.

The average percentage of accuracy obtained in this proposed method is 84.15%. As we go through each process in the methodology part, the pre-processing stage usually needs a method which has an ability to control the brightness of the original image. For instance, bottom-hat transformation is implemented in this system which has dark object with a bright background in the original fundus image.

The results in this stage starting from the extraction of green channel until the blood vessels extraction are perfectly fine as bottom-hat filter has succeed in enhancing the dark regions which correspond to MA and blood vessel are well extracted using Gaussian matched filter. In order to remove the extracted blood vessels, thresholding method is performed. Pixel value less than 0.09 is extracted while this value is remain fixed to be used in analyzing all images. However, in some images, this value produced inaccurate results where the blood vessels are not well-segmented producing a spurious objects that look similar to the MA. The resulting objects may disturb the process of extracting the microstructure features.

To extract the microstructures in the image, template learning using TEMPLAR algorithm is implemented. The total number of learning images are 9 where the dimension of each image are 30x30. The size of the image is chosen in order to exclude the noise in the template background. Thus, we only preserve the area of MA in each of the template data.

Next, wavelet coefficients are used to model the pattern and the background of the image where the large coefficients corresponding to the pattern of the image such as the edge while the small coefficients corresponding to image smoothing or denoising. In TEMPLAR algorithm, a low dimension of template is advantageous because it facilitates the pattern matching process by giving more weight to significant template coefficients, which is used for modeling the structure of the pattern, and less weight to surrounding clutter. In the result

sub-section, the synthesized images closely resemble the training data.

GMM is used for modeling wavelet coefficients by considering the local statistics of wavelet coefficients. This can be done by assuming the low state of the coefficient models the background and smooth regions while the high state models the pattern. In our method, GMM managed to distinguish this pattern and background image. However, the results of the pattern image still contain large-dot structures which are different from the properties of MA. This problem occurs possibly due to the less number of template data used in the learning process. Thus, missed detection of true features may occurred.

The evaluation of the system performance is done by computing the number of TP and FN to calculate the sensitivity. The improvement can be achieved by decreasing the false detection of MA. Thus, emphasizing on template training is needed in order to extract the microstructure features efficiently by introducing a large number of template data that covered all the properties of MA.

VI. CONCLUSION

The automated detection of the MA grants various challenges in realizing the objectives of this research. The MA candidates are difficult to be distinguished from the background variation as the shape, texture and size of the candidates are quite similar with the other types of lesions such as hemorrhage. Besides, the structure of blood vessel in fundus image can be one of the limitation in detection of MA.

Therefore, in this research, several filters and template learning methods have been used in order to segment the true MA in fundus image. As the summary of the methodology, the green component of color image is extracted, the contrast adjustment is performed, the blood vessel is then removed by using Gaussian matched filter and the wavelet based on Gaussian mixture model is performed. Next, the results obtained from previous methods are used to perform the Laws' filtering and finally statistical evaluation is conducted in order to evaluate the system performance. The results showed that the average percentage of TP is 84.15% while average percentage of FN is 15.85%.

In order to improve the system performance, manual marking of the raw image for the purpose of comparing the final image and the manually marked image should be done by experts. Besides, more samples of MA should undergo the template learning as we only proposed nine images for learning process. If more number of training images are used in template learning, better results can be achieved in distinguishing the pattern and background of the fundus image.

ACKNOWLEDGMENT

The research was made possible by the funding of the Ministry of Higher Education (MOHE) Malaysia, Technical University of Ilmenau (TUIL) and Universiti Teknologi Malaysia (UTM) under the Research University Tier 1 Grant (vote 12H72).

REFERENCES

[1] S. Jiménez, P. Alemany, F. Núñez Benjumea, C. Serrano, B. Acha, I. Fondón, F. Carral, and C. Sánchez, "Automatic detection of microaneurysms in colour fundus images for diabetic retinopathy screening," Arch. la Soc. Española Oftalmol. (English Ed., vol. 86, no. 9, pp. 277–281, 2011.

[2] T. Walter, P. Massin, A. Erginay, R. Ordonez, C. Jeulin, and J. C. , "Automatic detection of microaneurysms in color fundus images," Med. Image Anal., vol. 11, no. 6, pp. 555–566, 2007.

[3] G. Mahendran, R. Dhanasekaran, and K. N. Narmadha Devi, "Identification of exudates for Diabetic Retinopathy based on morphological process and PNN classifier," Int. Conf. Commun. Signal Process. ICCSP 2014 - Proc., pp. 1117–1121, 2014.

[4] D. Vallabha, R. Dorairaj, K. Namuduri, and H. Thompson, "Automated detection and classification of vascular abnormalities in diabetic retinopathy," Proc. Thirty-Eighth Asilomar Conf. Signals, Syst. Comput., vol. 2, pp. 1625–1629, 2004.

[5] C. X. Jayaseelan, "Early Detection of Microaneurysms Using Retinal Fundus Images With Removed Blood Vessel Analysis," vol. 4, no. 1, pp. 1–10, 2015.

[6] A. D. Fleming, S. Philip, K. A. Goatman, J. A. Olson, and P. F. Sharp, "Automated microaneurysm detection using local contrast normalization and local vessel detection," IEEE Trans. Med. Imaging, vol. 25, no. 9, pp. 1223–1232, 2006.

[7] M. García, C. I. Sánchez, M. I. López, A. Díez, and R. Hornero, "Automatic detection of red lesions in retinal images using a multilayer perceptron neural network.," Conf. Proc. ... Annu. Int. Conf. IEEE Eng. Med. Biol. Soc. IEEE Eng. Med. Biol. Soc. Annu. Conf., vol. 2008, pp. 5425–8, 2008.

[8] J. P. Bae, K. G. Kim, H. C. Kang, C. B. Jeong, K. H. Park, and J. M. Hwang, "A study on hemorrhage detection using hybrid method in fundus images," J. Digit. Imaging, vol. 24, no. 3, pp. 394–404, 2011.

[9] Yamuna, T., and S. Maheswari. "Detection of abnormalities in retinal images." Emerging Trends in Computing, Communication and Nanotechnology (ICE-CCN), 2013 International Conference on. IEEE, 2013.

[10] C. Scott and R. Nowak, "TEMPLAR: A Wavelet-Based Framework for Pattern Learning and Analysis", IEEE Transactions on Signal Processing, vol. 52, no. 8, pp. 2264-2274, 2004.

[11] M. Tamilarasi and K. Duraiswamy, "Automatic detection of microaneurysms using microstructure and wavelet methods," vol. 40, no. June, pp. 1185–1203, 2015.

[12] "Wavelet,"techtarget, [Online]. Avalaible: http://whatis.techtarget.com/definition/wavelet. [Accessed 22 February 2016]

[13] K. N. Ramamurthy, J. J. Thiagarajan, and A. Spanias, "Template Learning using Wavelet Domain Statistical Models," Res. Dev. Intell. Syst. XXVI, pp. 179–192, 2010.

[14] M. T. Suzuki, Y. Yaginuma, and H. Kodama, "A 2D Texture Image Retrieval Technique Based on Texture Energy Filters," IMAGAPP 2009 - Int. Conf. Imaging Theory Appl., no. 1, pp. 145–151, 2009.